Provisional chapter

Recent Progress in the Understanding and Manipulation of Morphology in Polymer: Fullerene Photovoltaic Cells

Gabriel Bernardo and David G. Bucknall

Additional information is available at the end of the chapter

http://dx.doi.org/10.5772/51115

1. Introduction

The morphology of the active layer in OPV devices is widely recognized as being crucial for their photovoltaic performance [1-4]. The physics of the system dictates that excitons must dissociate efficiently at a donor-acceptor interface, and that sufficient pathways for charge transport to the electrodes are also required. Conjugated polymer crystals are considered to be the primary hole carrier and thus are essential for effective charge transport. With this in mind, the ideal morphology for an organic photovoltaic BHJ film was often considered until a few years ago to be a bicontinuous, interpenetrating network morphology composed of pure P3HT and pure PCBM phases, with both phases of order ~20 nm in size [5, 6] and numerous cartoon depictions have helped to propagate this view, as the one shown in Figure 1.

In this idealized model, the two pure phases of donor and acceptor within the bulk heterojunction are interdigitated in percolated highways with an average length scale of around 10-20 nm, equal to or less than the exciton diffusion length, to ensure exciton dissociation and high mobility charge carrier transport with reduced recombination. Furthermore, a pure donor phase at the hole collecting electrode and a pure acceptor phase at the electron collecting electrodes should exist in order to minimize the losses by recombination of opposite charges or acting as diffusion barriers for the opposite sign charge carriers at the respective electrodes. The presence of mixed phases in these BHJ were considered to be counterproductive to device performance, since isolated molecules could act as traps for separated charges and centers for charge recombination within the percolation pathways.

Many efforts have used this ideal model to design studies that examine the effect of the chemical structure of conjugated polymer, composition, and processing methods on the abil-

ity to achieve this ideal interpenetrating two-phase system [1]. Furthermore, when describing the device physics of such organic photovoltaic devices, theoretical models have been developed which mainly relied on the assumption that the components existed as two separated pure phases [7-10].

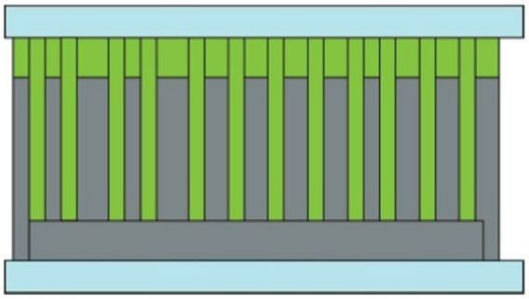

Figure 1. The ideal structure of a bulk heterojunction solar cell as represented by Sariciftci *et al* [5]. "Reprinted with permission from (Chemical Reviews 107 (2007) 1324). Copyright (2012) American Chemical Society."

Experimentally, although several different techniques have been used to study the morphology of these systems, part of the difficulties in the past in determining the precise composition of phases, interfacial structure, and morphology of bulk heterojunctions has been the limitations of contrast between the phases. For instance in standard electron-based techniques, crystalline P3HT and PCBM offer sufficient contrast between those two phases; however their amorphous counterparts are almost indistinguishable. Consequently conventional x-ray diffraction methods are unable to probe the amorphous regions in these conjugated polymer-fullerene mixtures. On the other hand, AFM techniques only allow the study of the morphology of surfaces and this might be very different from the morphology of the underlying bulk of the film. Differential scanning calorimetry (DSC) and dynamic mechanical analysis (DMA) have also been used but they can only provide indirect information about the morphology of these BHJ. For these reasons, more recently neutron and soft x-ray scattering techniques have started being used to provide heretofore unavailable information concerning the bulk morphology of these bulk heterojunctions. Additionally techniques utilizing specific atomic or group specific contrast such as secondary ion mass spectroscopy (SIMS) have added further information to the growing wealth of morphological information about BHJs. One clear advantage on the use of neutrons lies in the fact that for instance in the case of P3HT/PCBM systems, the scattering length density (SLD) difference between P3HT (0.83×10^{-6} Å^{-2}) and PCBM (4.3×10^{-6} Å^{-2}) is sufficiently high, and no additional deuteration of one component is necessary.

Over approximately the last five years a reinterpretation of the existing idealized model has lead to a new understanding on the thermodynamics and the morphology of these bulk heterojunction systems. This chapter reviews some of the relevant literature relating to this new

http://dx.doi.org/10.5772/51115

emerging understanding with concentration on the system of P3HT and PCBM, which has been the most widely studied OPV system to date.

2. The Thermodynamics and Phase Behavior of Conjugated Polymer-Fullerene Systems

Until a few years ago, the conventional wisdom was that the most widely studied OPV system of P3HT:PCBM was a simple two phase bulk heterojunction with well-defined interfaces between regions of approximately pure P3HT and pure PCBM. Then, from 2008 onwards several works in the literature began to show that this model was deficient in a number of ways since it did not account for the phase behavior of the mixtures or explain what the interface was between the phases or the two electrode interfaces. However, the results reported are often contradictory or conflicting as explained below.

One of the early studies to refute the concept of simple pure two phase behavior in BHJ systems was made by Muller *et al.* [11], who studied the phase behavior of PCBM with P3BT, P3HT and P3DDT using a combination of DSC, optical microscopy and X-ray diffraction (XRD) and related this to the solar cell efficiency for a series of devices with different blend compositions. These binary systems were shown to feature simple eutectic phase behavior (Figure 2(a)), with a eutectic composition of 35 wt% PCBM in the PCBM:P3HT system, and that the optimum composition for device performance is slightly hypoeutectic when expressed in terms of the polymer component.

Additional studies by Kim *et al.* [12], again using a combination of XRD and DSC, investigated the phase behavior of PCBM with P3HT, MDMO-PPV and MEH-PPV. They observed both P3HT melting point depression and glass transition temperature elevation in the P3HT:PCBM blends as a function of increasing PCBM wt%. However, as shown in Figure 2, the phase diagram they obtained differs from that of Muller *et al.* [11]. The determined solubility limits of PCBM in P3HT (Figure 2(b)), MDMO-PPV and MEH-PPV were 30, 40 and 50 wt% respectively. By measuring field effect conduction in transistors, a strong correlation was found between the phase behavior and the charge transport in the studied conjugated polymer/fullerene blends with hole-only transport being observed below the solubility limit and ambipolar transport at higher PCBM fractions.

A further measurement of the phase diagram of P3HT:PCBM blends was made by Zhao *et al.* [13] (Figure 2(c)) using conventional and modulated temperature DSC (DSC and MTDSC). Again the phase behavior differs from both Muller *et al* and Kim *et al*. Zhao and co-workers observed a single glass transition temperature (T_g) for all compositions, which increases with increasing concentration of PCBM from 12.1ºC for pure P3HT to 131.2ºC for pure PCBM. It was found that the film morphology of the blends results from a dual crystallization behavior in which the crystallization of each component is hindered by the other component. The phase diagram also showed that the morphology of the blends with 45-50 wt% PCBM, whilst giving the highest device performance, is intrinsically unstable at the desired maximum operating temperature of 80ºC, as the T_g is less than 40ºC. More recently, the

same authors investigated the phase behavior of PCBM blends with different PPV polymers [14] using these same techniques together with rapid heat-cool calorimetry (RHC). They observed the occurrence of liquid-liquid phase separation in the molten state of MDMO-PPV:PCBM and high T_g-PPV:PCBM blends, as indicated by the coexistence of two T_{gs} for blends with a PCBM weight fraction of around 80 wt% which contrasted to the P3HT:PCBM blends where no phase separation was observed in the molten state [13].

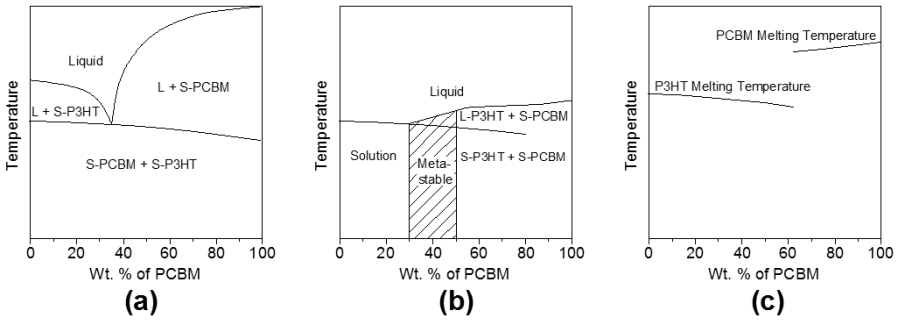

Figure 2. Phase diagrams of the system P3HT:PCBM as reported by Muller *et al* [11] (a); Kim *et al* [12] (b) and Zhao *et al* [13] (c).

Hopkinson *et al.* [15] also measured the phase diagram of P3HT:PCBM blends using DMTA and GI-WAXS. Evidence for a transition to a phase separated state is observed at PCBM concentrations greater than 70 wt% and the T_g of the blends increases from ~40ºC for pure P3HT to ~70ºC for a PCBM loading of 65 wt% and then drops between 70 and 75 wt% indicating phase separation. Interestingly, this T_g variation differs considerably from the corresponding variation reported by Zhao *et al.* [13]. By varying degrees of crystallinity of P3HT, Woo *et al.* [16] were able to control phase segregation in P3HT/PCBM mixtures and have shown that under the same annealing conditions, highly regioregular (RR) P3HT induces a larger extent of phase segregation (i.e., larger domains of pure phases) in a blend film with PCBM than lowly regioregular P3HT. This makes sense, since without co-crystallization the fullerenes can only exist in the amorphous regions of the polymer.

The effects of polymer crystallinity on miscibility have also been studied for P3HT and MDMO-PPV blended with PCBM by Collins *et al.* [17]. The miscibility curves for the P3HT:PCBM system obtained from NEXAFS measurements are shown in Figure 3. All systems show an increasing miscibility of PCBM with temperature, suggesting an upper critical solution temperature (UCST) for the binary phase diagram. Both the middle and high-RR grades of P3HT exhibit very similar levels of PCBM miscibility starting at 3% and 4% concentration at 120 ºC, respectively, up to approximately 10% at 180 ºC. Contrasting this is the regiorandom grade of P3HT that display much larger miscibility levels of 16-22%. Their results also showed that, while no intercalation occurs in P3HT crystals, amorphous portions of P3HT and MDMO-PPV contain significant concentrations of PCBM after annealing, calling into question mod-

http://dx.doi.org/10.5772/51115

els based on pure phases and discrete interfaces. Furthermore, depth profiles of P3HT/PCBM bilayers have been measured using SIMS and the results obtained revealed that even short annealing causes significant inter-diffusion of both materials, showing that under no conditions do pure amorphous phases exist in BHJ or annealed bilayer devices.

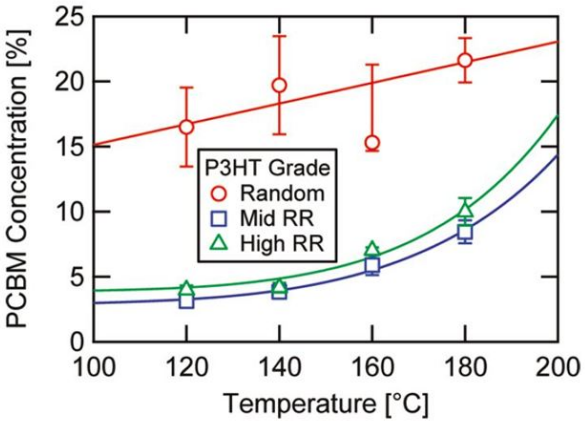

Figure 3. Miscibility phase diagram for P3HT mixed with PCBM according with Collins *et al.*[17]. "Reprinted with permission from (Journal of Physical Chemistry Letters 1 (2010) 3160). Copyright (2012) American Chemical Society."

Small-angle neutron scattering (SANS) studies on 1:1 P3HT:PCBM blend thin films by Kiel *et al.* [18] examined the change in scattering and consequently the location of PCBM upon thermal annealing (at 140 ºC for 20min). They found that after thermal annealing PCBM is soluble in the P3HT matrix up to a concentration of ~15-16 vol%. Although the data were not able to conclusively show that the dissolved PCBM was located in the amorphous P3HT, the authors suggested this as the probable location. They also observed that annealing has the effect of increasing the PCBM agglomeration and domain size and volume fraction suggesting a coarsening of the phase separated morphology.

Recently, Kozub *et al.* [19] have combined energy-filtered transmission electron microscopy (EFTEM) with grazing incidence small-angle X-ray scattering (GISAXS), to study the morphology evolution in P3HT/PCBM mixtures. They found that a significant amount of amorphous polymer exists as a homogeneous polythiophene-fullerene mixture. Elemental analysis of the amorphous regions demonstrated partial miscibility of P3HT and PCBM. They have also determined the χ parameter in P3HT-PCBM mixtures by measuring the melting point depression of P3HT in P3HT:PCBM mixtures. Through differential scanning calorimetry, they have obtained an estimate of the Flory-Huggins interaction parameter, χ, using Equation 1:

$$\frac{1}{T_m} + \frac{1}{T_m^0} = \frac{R}{\Delta H_f}\frac{v_m}{v_s}\left(\phi_s - \chi\phi_s^2\right) \quad (1)$$

where T_m is the melting point at a solvent (i.e. PCBM) volume fraction ϕ_s, T_m^0 is the melting point of pure polymer, R is the ideal gas constant, ΔH_f is the heat of fusion of polymer obtained from the melting endotherm, v_m is the monomer molar volume of polymer ($v_{m,P3HT}$ = 151 cm^3/mol) and v_s is the solvent molar volume ($v_{s,PCBM}$ = 607 cm^3/mol). Fitting Equation 1 to the melting point data shown in Figure 4(a) with χ as the only adjustable parameter yielded $\chi = 0.86 \pm 0.09$. Based on the assumption of Flory-Huggins free energy of mixing for polymer solutions, they obtained the spinodal, shown in Figure 4(b). The combination of the spinodal and χ allowed for the determination of the miscibility of amorphous P3HT:PCBM mixtures. They found that for P3HT concentrations greater than 0.42 by volume, the mixtures are miscible and this miscibility suppresses fullerene crystallization. They therefore concluded that the intricate mesoscopic structure of P3HT/PCBM mixtures present in 1:1 by mass mixtures (ϕ_{P3HT}= 0.58), commonly reported in the literature and critical for device performance, is not a result of demixing of the amorphous phases, but instead, must be a consequence of polymer crystallization.

Small-angle x-ray scattering (SAXS) studies of the phase separation of P3HT-PCBM thick films showed that a bulk heterojunction system blend of 1:0.7 P3HT:PCBM is not just a simple two-phase system with well-defined interfaces [20]. As other workers have shown the phase behavior was shown to be a much more complicated system incorporating regions of crystalline P3HT and PCBM, and a mixed phase of amorphous P3HT and PCBM. The phase separation length scale was found to be ~25 nm both before and after thermal annealing. The thermal annealing was also shown to cause a reduction in the phase separation associated with diffusion of PCBM into the amorphous P3HT, as previously also reported by Kiel *et al.* [18].

The influence played by the electrode interfaces on BHJ phase behavior has been studied by Chen *et al.* [21] on the multicomponent P3HT:PCBM system. Small angle neutron scattering and electron microscopy showed that a nanoscopic, bicontinuous morphology develops within seconds of annealing at 150 ºC and coarsens slightly with further annealing. P3HT and PCBM are shown to be highly miscible, to exhibit a rapid interdiffusion, and to display a preferential segregation of one component to the electrode interfaces.

Yin *et al.* [22] have also used SANS to study the bulk morphology of P3HT/PCBM samples prepared by drop casting a solution on a heated (~110ºC) quartz disk window (to accelerate drying). Blends of PCBM and P3HT were studied and the effects of composition and thermal annealing at 150 ºC on the resultant morphology and interfacial structure were examined. The SANS results indicate that P3HT and PCBM form homogeneous mixtures up to ~20 vol % PCBM, which was assigned as the approximate miscibility limit. At all PCBM fractions between 10 and 50 vol%, the resultant matrix also contains pure (crystalline) P3HT. At higher PCBM loadings, PCBM phase separates to form larger domains. In the system with 50 vol% PCBM, i.e. the system which is more representative of the active layer in organic photovoltaics, neutron scattering shows that there exist at least three coexisting phases; pure P3HT and PCBM phases, and a mixture of amorphous PCBM and P3HT that serves as the surrounding matrix. A simple geometric calculation indicates that the PCBM molecules in the amorphous phase are sufficiently close to allow charge transport, i.e. 4.3 Å at Φ =

http://dx.doi.org/10.5772/51115

15% loading and 3.3 Å at Φ = 20% fullerene loading. These distances are consistent with intermolecular charge transport models verifying therefore the ability of this morphology to create significant photocurrent when illuminated. The morphological model indicated by the SANS analysis is of "rivers and streams", as the PCBM/P3HT amorphous matrix contains an abundance of donor/acceptor interfaces resulting in an efficient dissociation of excitons. These charges then "flow" in the streams of PCBM or P3HT within the amorphous phase to the larger pure PCBM (electrons) or P3HT (holes) phases, which act as "rivers" to transport the charges to the electrodes. This efficient charge mobility morphology exists due to the extended miscibility of PCBM in P3HT, which is required to create sufficient close packing in the amorphous phase to allow charge transport in the "streams". Their proposed mechanism also explains the large difference in efficiency between P3HT/C_{60} and P3HT/PCBM bulk heterojunctions, where the immiscibility of C_{60} in P3HT presumably inhibits the formation of a morphology that allows effective charge transport to the "rivers".

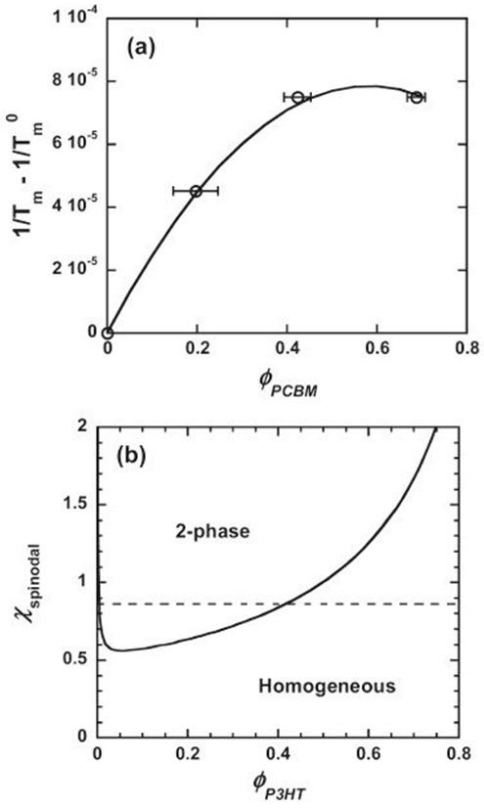

Figure 4. Estimate of the miscibility from measurements of the melting point depression, as described by Kozub *et al.* [19]. (a) Melting point depression of P3HT as a function of PCBM volume fraction, Φ_{PCBM}, obtained from DSC experiments. The solid line is from eq 1 with $\chi = 0.86$. Error bars represent the uncertainty in composition due to the limited

accuracy of the scale. (b) Spinodal as a function of P3HT volume fraction, Φ_{P3HT}, obtained by modeling P3HT:PCBM mixtures as polymer solutions with MWP3HT = 50 000 g/mol. The dotted line denotes $\chi = 0.86$, and in combination with the spinodal indicates that homogeneous P3HT:PCBM mixtures are unstable for P3HT < 0.42."Reprinted with permission from (Macromolecules 44 (2011) 5722). Copyright (2012) American Chemical Society."

Treat *et al.* [23] have used a bilayer of P3HT and PCBM, as a model system, to develop a more complete understanding of the miscibility and diffusion of PCBM within P3HT during thermal annealing. Fast interdiffusion of these two components was observed when annealed at 150 ° C for 30 s confirming the results of Che *et* al. [21]. This interdiffusion resulted in a homogeneous blend with an estimated diffusion coefficient of 3×10^{-10} cm^2 /s. The fact that there is a clear drive towards a homogeneous mixture of P3HT and PCBM from a distinctly heterogeneous structure strongly suggests that PCBM (molecular or aggregated species) is dispersible in disordered P3HT under typical annealing conditions of BHJ OPV. The authors estimate that PCBM has a concentration greater than 40 wt% in P3HT, which is consistent with previously reported estimates for bulk samples. It was also shown that PCBM diffuses to the P3HT film without affecting the crystal size, structure, or orientation of P3HT, even at an equal P3HT:PCBM weight ratio. These results indicate that the fast diffusion occurs only through the disordered regions of P3HT and shows how favorable the mixing in this system is. This again opposes the previously held belief that phase-pure domains form in BHJs due to immiscibility of these two components. These results confirm that the BHJ film is comprised of a dispersion of aggregates of PCBM, molecularly dispersed PCBM in disordered P3HT, and crystallites of P3HT and suggests that the pure polymer domains widely thought to exist in BHJ films are, in fact, disordered solutions of crystalline and disordered polymer and amorphous fullerene.

A direct comparison between conventionally prepared P3HT/PCBM BHJs (C-BHJ) and an active layer created by solution processed, layer-by-layer, sequential deposition (layer evolved BHJ, LE-BHJ) has been studied by Moon *et al.* [24]. Following annealing at 100ºC for 10 min. both OPVs based on P3HT/PCBM LE-BHJ and C-BHJ films show similar device efficiencies and transport properties. Within the limits of contrast, cross-sectional TEM images show that the intermixing of polymer and fullerene within the active layer of both OPVs (LE-BHJ and C-BHJ) is identical. Therefore, despite being dramatically different in preparation, these two methods produce nearly identical nano-morphologies. This spontaneous formation of equivalent morphologies through multiple routes implies that the resulting BHJ nanostructure is the lowest energy state of the system.

A systematic study to understand how the P3HT molecular weight influences the P3HT/PCBM phase behavior and the corresponding device performance has been undertaken by Nicolet *et al.* [25]. The phase diagrams for all P3HT:PCBM binary blends were obtained using DSC, displaying a eutectic phase diagram in all cases with a eutectic point found to decrease from 65 to 50 wt % for P3HT molecular weights increasing between 9.6 k and 60 k g/mol, respectively.

Molecular mixing in P3HT/PCBM thin films annealed at 140ºC was also the focus of a grazing incidence small-angle neutron scattering (GISANS) study by Ruderer *et al.* [26], which utilized a detailed analysis based on the distorted wave Born approximation (DWBA). A

http://dx.doi.org/10.5772/51115

broad range of compositions from 9 to 67 wt % PCBM content were investigated. The structure size obtained associated with the distance between PCBM domains, is found to be broadly distributed around 80 nm for systems with a small PCBM content of 9 wt % (see Figure 5(a)). For the systems with higher PCBM content, the distance was revealed to be constant at about 20 nm, which is in the range of the predicted exciton diffusion length and therefore beneficial for charge generation. While most analyzing methods are only able to extract overall structural length scales, the use of advanced modeling reveals much more detailed information. To fit the scattering data of such a complex system, up to three phase types associated with different PCBM domains have to be incorporated in the model. Over all blend ratios, large PCBM domains (Figure 5(a), triangles) with a radius of 100–200 nm are observed with low frequency (less than 0.05%). Much more frequently observed (>90%) smaller PCBM domains (Figure 5(a), squares), dominate the morphology. Their radius ranges from 3 to 10 nm with the maximum object size at a PCBM content of 50 wt %, which is in the range of the blend ratio where typically the most efficient P3HT/PCBM solar cells are found. For the systems with 25 and 33 wt % PCBM content, an additional PCBM domain with a radius in the range of 16-18 nm was observed again with low probability (<8%). Such an additional PCBM domain size might indicate a non-equilibrium morphology. The volume fraction of the molecularly dispersed PCBM, Φ_{PCBM}, a function of the overall PCBM content (see Figure 5(b)) shows that for the 9 wt % PCBM content films, a very low amount of molecularly dispersed PCBM is found. However, P3HT/PCBM films with a higher overall PCBM content (between 5 and 15 vol %) show molecularly dispersed PCBM.

As discussed above, the thermodynamics and phase behavior of conjugated polymer/fullerene systems is very complex and except in specific examples (such as P3HT/PCBM) it is still poorly understood. Even in the highly studied example of P3HT/PCBM there are conflicting results about the phase behavior. For example while some consider that these systems have an eutectic type of phase behavior [11-13] (as is usually found in metal mixtures and salt mixtures), others [19] are more in favor of the classical Flory-Huggins phase behavior common in amorphous polymer systems [27]. There is also disagreement in the P3HT/PCBM miscibility limits (i.e. in the amount of molecularly dispersed PCBM in the P3HT phase) reported in the literature. For instance, while Kozub *et al* [19] reported a value of > 42% vol % P3HT, Yin *et al.* [22] reported a miscibility limit of 20 vol % of PCBM molecularly dispersed in P3HT, and Ruderer *et al.* [26] reported a molecularly dispersed PCBM content of up to 35% in the amorphous P3HT phase. Despite these conflicting arguments, all of these studies are consensual in that all of them show clearly that the ideal model of pure phase separated donor and acceptor domains, as shown in Figure 1, is unattainable using the standard processing techniques (spin-coating followed by annealing) and therefore in order to explain the efficiencies of the currently existing devices, a paradigm shift in the physics behind device operation may be required, as has been suggested by some authors [17, 22].

In most of the studies described above, the main focus has been the study of the thermodynamics of the bulk and therefore the experimental samples were thick enough to avoid any relevant effect from the substrate's surface energy. It is however known that in very thin polymer films (~100 nm) as used in OPVs, the thin film morphology and phase behavior is

also affected by the substrate's surface energy. This phenomenon has also been the object of intense research and it is known that the substrate's free energy can induce vertical phase segregation (normal to the substrate's surface). However, just like reports of bulk BHJ behavior there are also contradictory reports in the literature concerning the effect of the substrate's surface energy on the final film morphology.

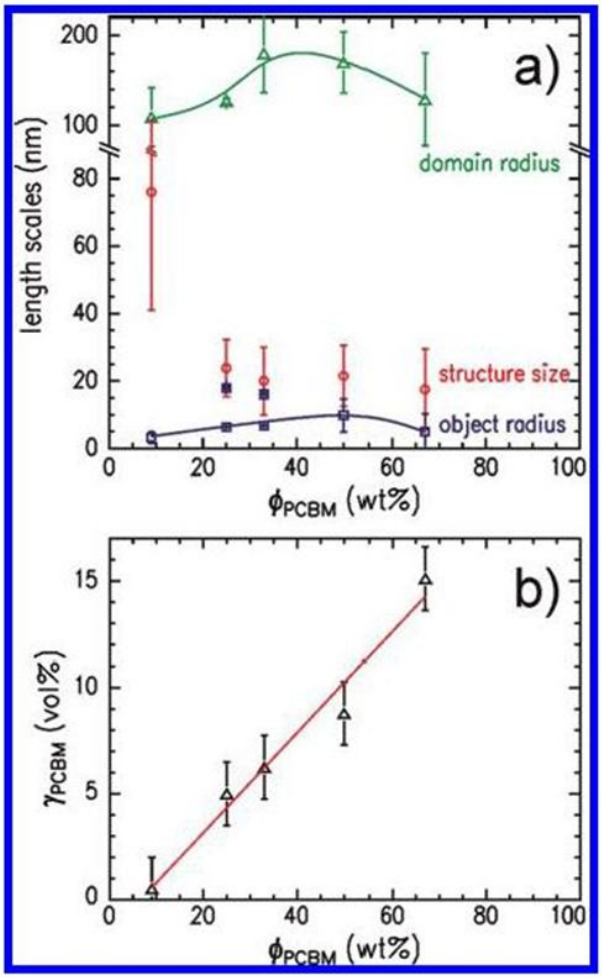

Figure 5. a) Distances (structure size) and small (object radius) and large PCBM domains (domain radius) used for the simulations of the GISANS data depending on the PCBM content [26]. The error bars represent the distribution of these lengths. (b) Fraction of the molecularly dissolved PCBM in the P3HT phase depending on the overall PCBM content. The solid lines are guides to the eyes. "Reprinted with permission from (Journal of Physical Chemistry Letters 3 (2012) 683). Copyright (2012) American Chemical Society."

http://dx.doi.org/10.5772/51115

The compositional depth profiles in thin films of APFO-3:PCBM blends spin-coated from chloroform solutions onto silicon has been studied by Björström *et al.* [28] using dynamic secondary ion mass spectrometry (D-SIMS). Vertical phase segregation was found to be caused by specific interactions between the substrates and the components of the APFO-3:PCBM mixtures. By changing the substrate from silicon to gold it was shown that the composition profile near the substrate interface varied. Later work by Campoy-Quiles *et al.* [29] also showed that changing the surface energy of a substrate can change the concentration profile of PCBM and, in the case of thermal annealing, cause PCBM to cluster together on an SiO_2 substrate.

Vertical segregation behavior in P3HT:PCBM (1:1) blend films were also studied by Kim *et al.* [30] using a glow discharge spectrometer equipped with a RF plasma (Ar ion) depth profiling system. They found that the relative distribution of P3HT and PCBM molecules changed considerably by thermal annealing, with increasing PCBM and P3HT enrichment close to the electron-collecting (Al) and to the hole-collecting (PEDOT:PSS/ITO) electrodes, respectively. Even in the absence of the Al electrode P3HT enrichment at the free (air) surfaces and abundance of fullerene derivatives at the organic/substrate interfaces was also observed by Xu *et al.* [31]. The vertical phase separation in this system was attributed to the surface energy difference of the components and hence their differential interaction with the substrates.

The importance of film thickness has been investigated by Verploegen *et al* [32] who showed that very thin films (20 to 25 nm thick) of P3HT:PCBM 1:3 display dewetting when annealed at 160ºC. Films of 75 nm thickness of the same composition when annealed did not dewet, but showed some signs of crystallization induced phase separation. Using neutron reflectivity (NR) Kiel *et al.* [33] showed that in a P3HT:PCBM BHJ, although the concentration profile is complicated through the film thickness, the PCBM concentrated at the substrate interface and also close to, but not at, the air interface where the aluminum counter-electrode was deposited. Upon annealing, however, the PCBM accumulates at the air interface creating an improved pathway for electrons to leave the device through the deposited metal electrode. PCBM migration upon thermal annealing is a clear indicator that it is in a kinetically trapped state upon spin coating and has some mobility within the device.

Further NR studies of morphology of the P3HT:PCBM thin films either freshly cast, or after solvent and thermally annealing have been made by Parnell *et al.* [34]. They found that the freshly cast films have a surface layer that is relatively depleted in PCBM, while being relatively rich in PCBM at the film–substrate interface. Solvent annealing was shown to have little effect on the PCBM distribution within the film, however thermal annealing increased the PCBM concentration at the surface to a level found in the bulk of the film. Neutron reflectivity measurements also suggest that the free surface of the films (i.e. without top metal electrode layer) undergo surface roughening when subject to solvent vapor and thermal annealing, a conclusion verified by scanning probe microscopy. It was presumed that the PCBM-depleted layers found in 'as-cast' P3HT/PCBM thin films are partly responsible for their relatively poor performance in OPV devices, and that thermal annealing OPV devices improves device efficiency not only by the creation of a percolated PCBM network, but also by improving electron extraction via increasing the PCBM concentration next to the device cathode.

The use of ToF-SIMS has been able to add to the morphological model derived by NR measurements by examining both the vertical as well as the lateral distribution of PCBM and P3HT in BHJ films [35]. In 150 nm thick films spun coated from a 1:1 weight ratio of P3HT:PCBM chlorobenzene solutions, ToF-SIMS imaging showed that the lateral phase separation (within the limit of the micron resolution of SIMS imaging) was similar before and after an annealing treatment at 140^{o}C for 30 min. However, depth profiling clearly shows a vertical phase separation of P3HT:PCBM on the pristine blend (before annealing), with a higher concentration of PCBM close to the PEDOT:PSS interface. On the other hand, after annealing, the cross-sectional images of PCBM and P3HT are both uniform along the vertical axis showing that the annealing treatment suppresses the vertical phase segregation. Using low voltage, high resolution TEM, Beal *et al.* [36] revealed some details of the mechanism of PCBM domain migration associated with the vertical segregation within P3HT:PCBM solar cells by giving direct confirmation of P3HT and PCBM crystallization.

Xue *et al.* [37] have used the variation of the post-annealing cooling rate to create a series of "snapshots" of the reorganization processes that occur upon annealing. P3HT:PCBM blend devices exhibit a complex vertical stratification of both crystallinity and blend composition. Using a combination of UV-vis spectroscopy, XRD, NEXAFS, AFM, and contact angle measurements, they showed that annealing resulted in the formation of three distinct vertical layers. Diffusion of PCBM from the interfaces into the bulk of the film results in the formation of (a) a P3HT rich substrate interfacial (wetting) layer, (b) a homogeneous 'bulk'central layer, and (c) a P3HT-rich air interfacial (capping) layer. The orientation of the P3HT molecules was shown to vary from *c*-axis P3HT alignment in the wetting layer at the substrate interface to an *a*-axis aligned in the capping layer at the air interface and also in the bulk layer. The data showed that by slowing the post-annealing cooling rate devices with significantly enhanced efficiencies can be prepared. This improvement in device performance was correlated with the observed increased crystallinity and hence polymer alignment, and also phase segregation both at the interfaces and in the bulk film. In particular, they found that slow cooling resulted in an aligned interfacial active layer/substrate structure that is beneficial for charge transport.

Theoretical descriptions indicate a segregation preference for a typical photovoltaic device is where the donor (P3HT) is concentrated close to the substrate, and the acceptor (PCBM) next to the top surface, onto which the cathode (for example Al) is deposited. This distribution of components is expected to enhance the selectivity of the contacts towards one type of charge carrier and so reduce charge leakage. As discussed above, there are clearly contradictory results in the experimental literature concerning the exact nature of this vertical phase segregation. However, there is agreement that annealing leads to an increase of the PCBM concentration closer to the cathode [30, 33-35], and this has been pointed out as being one of the reasons for the improvement of device efficiencies that is usually observed upon annealing treatments. The timing of the annealing process, i.e. before or after the deposition of a metal electrode, is also known to influence the results. Post-production thermal annealing can improve the evolution of well-ordered nanoscale morphology because of a limitation of PCBM overgrowth, that is, due to the confinement effect.

http://dx.doi.org/10.5772/51115

3. Kinetic Considerations

As shown in Figure 2, Muller *et al.* [11] and Kim *et al.* [12] reported an eutectic composition (C_e) of Ce ≈ 35 – 40 wt% PCBM and Zhao *et al.* [13] a value of C_e≈ 60 wt% PCBM. However, whilst these authors were trying to extract the thermodynamic behavior of the blends, kinetic factors are clearly affecting the resulting observations. It is these types of discrepancies in observed phase behavior that highlights the difficulty in understanding the fundamental relationship between morphology and device performance. Although the morphology of the BHJ is ultimately determined by thermodynamic factors, the observed thin film morphology can be dominated by the kinetics of the film preparation methods and parameters used, including solvent evaporation/drying rates and by the kinetics of cooling after annealing. Herein lies some of the answer as to the reason for the contradictions in the observed phase behavior and morphology of these systems, since in putting together a device, the processing conditions between different groups often vary and also almost certainly do not allow the system to reach a global free energy minima and hence true a thermodynamic state. Changes to processing conditions are well known to make big variations in device performance, but there are also much subtler effects associated with the well-known irreproducibility in otherwise identical processing conditions, which are problematic for OPV development.

The effect of drying kinetics on the resultant P3HT:PCBM blend has a profound effect on the final device characteristics [38], where it was found that films dried slowly had better performance characteristics (higher external quantum efficiency, higher power conversion efficiency, higher fill factor, and lower series resistance) than the rapidly dried films. The charge carrier mobility of holes and electrons in P3HT:PCBM thick films was shown to have more balanced transport properties and non-dispersive dynamics for the slowly dried films, where as the rapidly dried film displayed dispersive dynamics and unbalanced transport. All these differences in performance were explained by the rate of solvent evaporation, as fast solvent loss quenches the phase separation process, and conversely the longer the blend is mobile and contains solvent the more the mixture will proceed to a more phase separated state. Campoy-Quiles *et al.* [29] have studied the morphology changes induced by slow drying and vapour annealing and showed that the PCBM concentration profile changes as the spin-coating speed (and hence the rate of drying) is reduced. Slow drying has a qualitatively similar effect to thermal annealing, whereby the composition gradient becomes more pronounced and the surface-segregated PCBM concentration increases.

The time-dependent morphology evolution of blend films of P3HT and PCBM, was investigated by Jo *et al.* [39], using two different annealing treatments with different morphology evolution time scales, i.e. a high-temperature thermal annealing (150 ºC), and a room-temperature solvent annealing. Comparing the morphological changes of the blend films after the two annealing treatments, solvent annealing resulted in a more favorable BHJ morphology than thermal annealing. The poor BHJ morphology after thermal annealing under these experimental conditions was attributed to the relatively fast diffusion and aggregation of the PCBM molecules during P3HT crystallization, which interfered with the growth of the elongated fibrillar P3HT crystals and subsequent evolution of the well-ordered BHJ morpholo-

gy. These results are however, seemingly contradictory to those of Parnell *et al.* [34], suggesting that there are other factors that are contributing to the observed behaviors.

The reasons for the irreproducibility of the performance of P3HT:PCBM BHJ solar cells fabricated using nominally identical conditions has been investigated by de Villers *et al.* [40]. They showed that this irreproducibility is the result of the occurrence of vertical phase segregation of P3HT to the top surface, which is controlled by subtle factors in the kinetics of solvent evaporation during spin-coating. When this type of vertical phase separation occurs, electron extraction is hindered by the poor contact between the PCBM component of the BHJ and the cathode.

Wang *et al.* [41] have used in-situ ellipsometry and grazing incidence x-ray scattering (GIXS) to study molecular self-organization in P3HT and PCBM blend films in real time, during the drying process as they are cast from solution. They have identified three stages in film drying: (I) rapid solvent-evaporation, (II) moderate solvent-evaporation and rapid crystallization, and (III) slow solvent-evaporation and slow crystallization. They showed that the onset of fast crystallization commences when the volume fraction of P3HT:PCBM in a wet film reaches a critical volume fraction of 50%. The observed crystallization growth-mechanism is consistent with a heterogeneous nucleation process in which defects or impurities act as nucleation sites.

The rate of evaporation is clearly affected by the boiling point and vapor pressure of the solvents used. The influence solvent boiling point on the morphology and photovoltaic performance of P3HT:PCBMBHJ films produced via spin-coating, has been studied by Ruderer *et al*. [42]. The four solvents considered were chloroform (CF), toluene, chlorobenzene (CB) and xylene. Solar cells made using these solvents had different photovoltaic performances. Using a wide range of experimental techniques it was shown that solubility-driven cluster formation of PCBM occurred in these systems. In films made using solvents with poor solubility of PCBM many more clusters were formed. As-spun films showed no P3HT crystallinity, independent of the solvent used. After annealing, P3HT crystals formed with edge-on configuration relative to the substrate as the main orientation, with crystal lattice constants that were also independent of the solvent used. However the crystal sizes increased with increasing boiling point (i.e. decreasing evaporation rates) of the solvents used, which was attributed to the increased drying time during spin-coating and residual solvent in the BHJ films. For toluene-, CB-, and xylene-made films, lateral nanostructures were found. In the vertical direction P3HT enrichment layers were detected for toluene- and CB-made films and PCBM enrichment layers for the films made using toluene and xylene. Nevertheless films made using toluene, CB, and xylene showed similar photovoltaic performance. Conversely, films made using chloroform presented a layered structure with a disadvantageous material distribution, with the P3HT hole conductor at the top electrode and the PCBM electron conductor at the electron-blocking layer, consequently producing efficiencies that were significantly lower.

Schmidt-Hansberg *et al.* [43] have investigated the dynamics and thermodynamics of molecular ordering, in P3HT/PCBM mixtures, during film drying from 1,2-dichlorobenzene (DCB). The pathway through the phase diagrams of P3HT and PCBM solutions, as shown in

http://dx.doi.org/10.5772/51115

Figure 6, was compared with the structural changes during crystallization of the ternary P3HT:PCBM:solvent system observed in real time by grazing incidence x-ray diffraction (GIXD). It was shown that PCBM only crystallizes at the final stage of drying although its solubility limit is reached a very early stage of solvent evoporation.

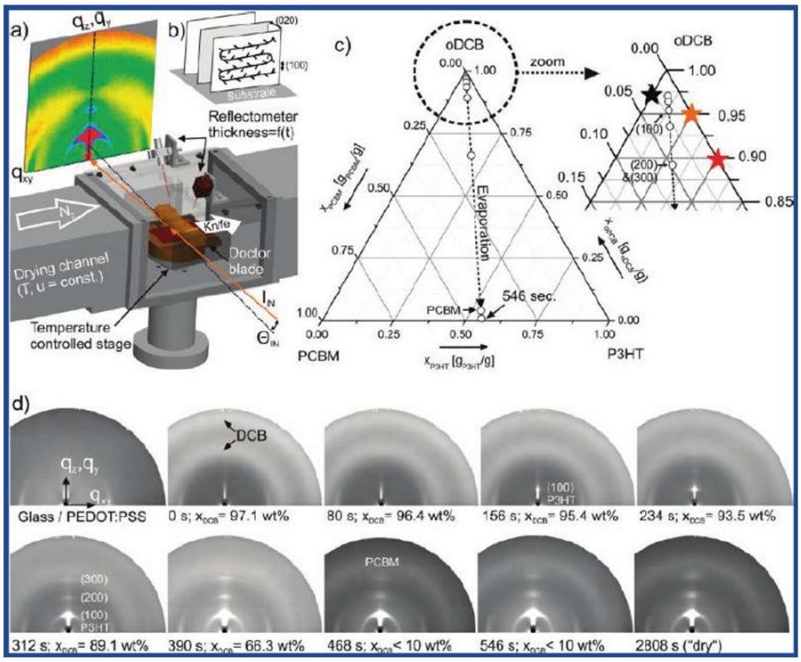

Figure 6. a) Schematic of the experimental setup for simultaneous real time GIXD and laser reflectometry of doctor-bladed thin films in a controlled drying environment. (b) Schematic of P3HT unit cell. (c) Ternary phase diagram of P3HT-PCBM-DCB; the star symbols denote phase transitions in the binary cases. From reference [43]. "Reprinted with permission from (ACS Nano 5 (2011) 8579). Copyright (2012) American Chemical Society."

Sobkowicz *et al.* [44] have measured the time- and temperature dependent aggregation of P3HT in o-dichlorobenzene solutions using rheometry and small-angle neutron scattering (SANS). They tried to set a starting point for understanding important aspects of morphology development in drying BHJ films. They found that the presence of PCBM dramatically slows the aggregation of P3HT in solution. Concentration and temperature dependencies were identified, with the latter being the more sensitive parameter. Analysis of the SANS data showed a strong affinity between P3HT and DCB with an interaction parameter that becomes more negative with increasing concentration, and elevated temperature dissolution suggesting UCST behavior in this polymer–solvent system. Modest cooling of P3HT solutions even in "good" solvents such as DCB resulted in rapid aggregation, although the aggregated solutions do not completely phase separate, but rather form physical gels consisting of anisotropic structures. An increase in solution modulus of several orders of

magnitude accompanies the aggregation and the pure polymer solution modulus becomes frequency-independent. Although the percent crystallinity in the aggregated solutions cannot be calculated directly from these results, it appears that the crystalline fraction is lower in the solutions with PCBM present. These results also lend insight into the film drying process and will ultimately lead to improved processing procedures in pursuit of an optimized morphology for bulk heterojunction devices.

The rate of cooling, after annealing, also has a dramatic influence on the final morphology of the film. A slower cooling rate leads to a greater extent of crystallization, when semi-crystalline polymers or crystalline nano-particles are involved. Despite this fact, only recently have some authors drawn attention to this important factor [37].

4. Conclusions

Recent detailed studies of the phase behavior of conjugated polymer:fullerene blends have begun to provide important information for understanding the property-processing relationships in organic solar cell blends. Until these studies conventional wisdom suggested that the P3HT:PCBM system was a simple two phase bulk heterojunction with well-defined interfaces between regions of pure P3HT and pure PCBM. The latest results clearly demonstrate that this assumption is not correct, but instead unequivocally show that BHJ materials are more complex systems incorporating regions of crystalline P3HT, PCBM, and intermixed regions of amorphous P3HT and PCBM. Upon annealing there is considerable interdiffusion of PCBM into the amorphous P3HT. It has also been shown that in the case of thin BHJ films (~100 nm) such as those used in OPVs, the substrate's surface energy can have a crucial role on the final morphology.

Furthermore, the kinetics as manifested in the processing routes and conditions can also play a dominant role in the observed structure/morphology. For all these reasons it is very difficult to predict the structure of the BHJ since apparently the same process used by different groups can end to with different results.

Whilst significant insight has been derived in understanding the behavior of a limited number of systems, with P3HT:PCBM the most widely studied system by far, there is still no predictive understanding in even this system. If technologically meaningful device efficiencies are to be achieved significant additional work must be undertaken to derive predictive capability for these complex BHJ systems. This will ultimately require a global effort of complementary experimental measurements combined with theoretical and computational modeling.

5. Nomenclature

AFM – Atomic Force Microscopy

BHJ – Bulk Hetero-Junction

http://dx.doi.org/10.5772/51115

DMTA – Dynamic Mechanical Thermal Analysis

GISANS - Grazing Incidence Small-Angle Neutron Scattering

GIXS – Grazing Incidence X-ray Scattering

GIWAXS/GIXD – Grazing Incidence Wide-Angle X-ray Scattering/x-ray diffraction

ITO – Indium Tin Oxide

MEH-PPV - poly [2-methoxy-5-(2-ethyl-hexyloxy)-1,4-phenylene-vinylene]

MDMO-PPV – poly(2-methoxy-5-(3′,7′-dimethyloctyloxy)-1,4-phenylenevinylene)

NEXAFS – Near-Edge X-ray Absorption Fine Structure

NR – Neutron Reflectivity

OPV – Organic Photo-Voltaic

P3HT – poly(3-hexylthiophene)

PCBM – phenyl-C61-butyric acid methyl ester

PEDOT:PSS – Poly(3,4-EthyleneDiOxyThiophene):Poly(StyreneSulfonate)

SANS – Small Angle Neutron Scattering

SAXS – Small-Angle X-ray Scattering

SIMS – Secondary Ion Mass Spectrometry

TEM – Transmission Electron Microscopy

ToF-SIMS – Time-of-Flight Secondary Ion Mass Spectrometry

UCST – Upper Critical Solubility Temperature

UV-Vis – Ultra-Violet Visible

XRD – X-ray diffraction

WAXS – Wide-Angle X-ray Scattering

Acknowledgements

Gabriel Bernardo acknowledges financial support from the IPC's (Institute for Polymers and Composites) strategic project: "PEst-C/CTM/LA0025/2011" (Projecto Estratégico—LA 25—2011-2012—Strategic Project—LA 25—2011-2012).

Author details

Gabriel Bernardo[1*] and David G. Bucknall[2]

*Address all correspondence to: gabriel.bernardo@dep.uminho.pt

1 Institute for Polymers and Composites/I3N, University of Minho, Campus de Azurém, Portugal

2 Materials Science and Engineering, Georgia Institute of Technology, USA

References

[1] Hoppe, H., & , N. S. (2006). Sariciftci, Morphology of polymer/fullerene bulk heterojunction solar cells. *Journal of Materials Chemistry*, 16(1), 45-61.

[2] Hoppe, H., et al. (2004). Nanoscale morphology of conjugated polymer/fullerene-based bulk-heterojunction solar cells. *Advanced Functional Materials*, 14(10), 1005-1011.

[3] Chen, L. M., et al. (2009). Recent Progress in Polymer Solar Cells: Manipulation of Polymer: Fullerene Morphology and the Formation of Efficient Inverted Polymer Solar Cells. *Advanced Materials*, 1434-1449.

[4] Brady, M. A., Su, G. M., & Chabinyc, M. L. (2011). Recent progress in the morphology of bulk heterojunction photovoltaics. *Soft Matter*, 7(23), 11065-11077.

[5] Gunes, S., Neugebauer, H., & Sariciftci, N. S. (2007). Sariciftci, Conjugated polymer-based organic solar cells. *Chemical Reviews*, 107(4), 1324-1338.

[6] Saunders, B. R., & Turner, M. L. (2008). Nanoparticle-polymer photovoltaic cells. *Advances in Colloid and Interface Science*, 138(1), 1-23.

[7] Sylvester-Hvid, K. O., Rettrup, S., & Ratner, M. A. (2004). Two-dimensional model for polymer-based photovoltaic cells: Numerical simulations of morphology effects. *Journal of Physical Chemistry B*, 108(14), 4296-4307.

[8] Sylvester-Hvid, K. O., & Ratner, M. A. (2005). Simplified charge separation energetics in a two-dimensional model for polymer-based photovoltaic cells. *Journal of Physical Chemistry B*, 109(1), 200-208.

[9] Lei, B., et al. (2008). Quantifying the relation between the morphology and performance of polymer solar cells using Monte Carlo simulations. *Journal of Applied Physics*, 104(2), 024504.

[10] Meng, L. Y., et al. (2010). Dynamic Monte Carlo Simulation for Highly Efficient Polymer Blend Photovoltaics. *Journal of Physical Chemistry B*, 114(1), 36-41.

[11] Muller, C., et al. (2008). Binary organic photovoltaic blends: A simple rationale for optimum compositions. *Advanced Materials*, 20(18), 3510.

[12] Kim, J. Y., & Frisbie, D. (2008). Correlation of Phase Behavior and Charge Transport in Conjugated Polymer/Fullerene Blends. *Journal of Physical Chemistry C*, 112(45), 17726-17736.

[13] Zhao, J., et al. (2009). Phase Diagram of P3HT PCBM Blends and Its Implication for the Stability of Morphology. *Journal of Physical Chemistry B*, 113(6), 1587-1591.

[14] Zhao, J., et al. (2011). Phase behavior of PCBM blends with different conjugated polymers. *Physical Chemistry Chemical Physics*, 13, 12285-12292.

[15] Hopkinson, P. E., et al. (2011). A Phase Diagram of the P3HT PCBM Organic Photovoltaic System: Implications for Device Processing and Performance. *Macromolecules*, 44(8), 2908-2917.

[16] Woo, C. H., et al. (2008). The Influence of Poly(3-hexylthiophene) Regioregularity on Fullerene-Composite Solar Cell Performance. *Journal of the American Chemical Society*, 130(48), 16324-16329.

[17] Collins, B. A., et al. (2010). Molecular Miscibility of Polymer-Fullerene Blends. *Journal of Physical Chemistry Letters*, 1(21), 3160-3166.

[18] Kiel, J. W., Eberle, A. P. R., & Mackay, M. E. (2010). Nanoparticle Agglomeration in Polymer-Based Solar Cells. *Physical Review Letters*, 105(16), 168701.

[19] Kozub, D. R., et al. (2011). Polymer Crystallization of Partially Miscible Polythiophene/Fullerene Mixtures Controls Morphology. *Macromolecules*, 44(14), 5722-5726.

[20] Parnell, A. J., et al. (2011). Nanoscale Phase Separation of P3HT PCBM Thick Films As Measured by Small-Angle X-ray Scattering. *Macromolecules*, 44(16), 6503-6508.

[21] Chen, D., et al. (2011). P3HT PCBM Bulk Heterojunction Organic Photovoltaics: Correlating Efficiency and Morphology. *Nano Letters*, 11(2), 561-567.

[22] Yin, W., & Dadmun, M. (2011). A New Model for the Morphology of P3HT PCBM Organic Photovoltaics from Small-Angle Neutron Scattering: Rivers and Streams. *Acs Nano*, 5(6), 4756-4768.

[23] Treat, N. D., et al. (2011). Interdiffusion of PCBM and P3HT Reveals Miscibility in a Photovoltaically Active Blend. *Advanced Energy Materials*, 1(1), 82-89.

[24] Moon, J. S., et al. (2011). Spontaneous Formation of Bulk Heterojunction Nanostructures: Multiple Routes to Equivalent Morphologies. *Nano Letters*, 11(3), 1036-1039.

[25] Nicolet, C., et al. (2011). Optimization of the Bulk Heterojunction Composition for Enhanced Photovoltaic Properties: Correlation between the Molecular Weight of the Semiconducting Polymer and Device Performance. *Journal of Physical Chemistry B*, 115(44), 12717-12727.

[26] Ruderer, M. A., et al. (2012). Phase Separation and Molecular Intermixing in Polymer-Fullerene Bulk Heterojunction Thin Films. *Journal of Physical Chemistry Letters*, 3(6), 683-688.

[27] Eitouni, H. B., & Balsara, N. P. (2007). Thermodynamics of Polymer Blends. in J.E. Mark (Ed) Physical Properties of Polymers Springer , 339-356.

[28] Bjorstrom, C. M., et al. (2007). Vertical phase separation in spin-coated films of a low bandgap polyfluorene/PCBM blend- Effects of specific substrate interaction. *Applied Surface Science*, 253(8), 3906-3912.

[29] Campoy-Quiles, M., et al. (2008). Morphology evolution via self-organization and lateral and vertical diffusion in polymer: fullerene solar cell blends. *Nature Materials*, 7(2), 158-164.

[30] Kim, Y., et al. (2009). Distorted Asymmetric Cubic Nanostructure of Soluble Fullerene Crystals in Efficient Polymer:Fullerene Solar Cells. *Acs Nano*, 3(9), 2557-2562.

[31] Xu, Z., et al. (2009). Vertical Phase Separation in Poly(3-hexylthiophene): Fullerene Derivative Blends and its Advantage for Inverted Structure Solar Cells. *Advanced Functional Materials*, 19(8), 1227-1234.

[32] Verploegen, E., et al. (2010). Effects of Thermal Annealing Upon the Morphology of Polymer-Fullerene Blends. *Advanced Functional Materials*, 20(20), 3519-3529.

[33] Kiel, J. W., et al. (2010). Nanoparticle concentration profile in polymer-based solar cells. *Soft Matter*, 6(3), 641-646.

[34] Parnell, , et al. (2010). Depletion of PCBM at the Cathode Interface in P3HT/PCBM Thin Films as Quantified via Neutron Reflectivity Measurements. *Advanced Materials*, 22(22), 2444.

[35] Yu, B. Y., et al. (2010). Effect of Fabrication Parameters on Three-Dimensional Nanostructures of Bulk Heterojunctions Imaged by High-Resolution Scanning ToF-SIMS. *Acs Nano*, 4(2), 833-840.

[36] Beal, R.M., et al. (2010). The Molecular Structure of Polymer-Fullerene Composite Solar Cells and Its Influence on Device Performance. *Macromolecules*, 43(5), 2343-2348.

[37] Xue, B. F., et al. (2010). Vertical Stratification and Interfacial Structure in P3HT PCBM Organic Solar Cells. *Journal of Physical Chemistry C*, 114(37), 15797-15805.

[38] Li, G., et al. (2005). High-efficiency solution processable polymer photovoltaic cells by self-organization of polymer blends. *Nature Materials*, 4(11), 864-868.

[39] Jo, J., et al. (2009). Time-Dependent Morphology Evolution by Annealing Processes on Polymer:Fullerene Blend Solar Cells. *Advanced Functional Materials*, 19(6), 866-874.

[40] de Villers, B. T., et al. (2009). Improving the Reproducibility of P3HT PCBM Solar Cells by Controlling the PCBM/Cathode Interface. *Journal of Physical Chemistry C*, 113(44), 18978-18982.

http://dx.doi.org/10.5772/51115

[41] Wang, T., et al. (2010). The development of nanoscale morphology in polymer: fullerene photovoltaic blends during solvent casting. *Soft Matter*, 6(17), 4128-4134.

[42] Ruderer, M. A., et al. (2011). Solvent-Induced Morphology in Polymer-Based Systems for Organic Photovoltaics. *Advanced Functional Materials*, 21(17), 3382-3391.

[43] Schmidt-Hansberg, B., et al. (2011). Moving through the Phase Diagram: Morphology Formation in Solution Cast Polymer-Fullerene Blend Films for Organic Solar Cells. *Acs Nano*, 5(11), 8579-8590.

[44] Sobkowicz, M. J., et al. (2012). Effect of Fullerenes on Crystallization-Induced Aggregation in Polymer Photovoltaics Casting Solutions. *Macromolecules*, 45(2), 1046-1055.